

Gray Matter Based Spatial Statistics Framework in the 1-Month Brain: Insights into Gray Matter Microstructure in Infancy

Authors: Marissa A. DiPiero^{1,2}, Patrik Goncalves Rodrigues¹, McKaylie Justman¹, Sophia Roche¹, Elizabeth Bond¹, Jose Guerrero Gonzalez¹, Richard J. Davidson^{1,3,4,5}, Elizabeth M. Planalp⁶, Douglas C. Dean III^{1,7,8}

¹Waisman Center, University of Wisconsin–Madison, Madison, WI, USA

²Neuroscience Training Program, University of Wisconsin–Madison, Madison, WI, USA

³Department of Psychology, University of Wisconsin–Madison, Madison, WI, USA

⁴Center for Healthy Minds, University of Wisconsin–Madison, Madison, WI, USA

⁵Department of Psychiatry, University of Wisconsin–Madison, Madison, WI, USA

⁶Wisconsin Alzheimer's Disease Research Center, University of Wisconsin–Madison School of Medicine and Public Health, Madison, WI, USA

⁷Department of Pediatrics, University of Wisconsin–Madison, Madison, WI, USA

⁸Department of Medical Physics, University of Wisconsin–Madison, Madison, WI, USA

Address Correspondence to: Douglas C. Dean III
Waisman Center
University of Wisconsin–Madison
Madison, WI, USA, 53705
Tel. # +1 608.262.6706
Email: deaniii@wisc.edu

ORCID:

Douglas C. Dean III: <https://orcid.org/0000-0002-7057-1285>

Marissa A. DiPiero: <https://orcid.org/0000-0003-4585-1100>

Data Availability Statement: Data will be made available upon request.

Acknowledgements: We sincerely thank our research participants and their families who participated in this research as well as the dedicated research staff who made this work possible. This work was supported by grants by the National Institutes of Mental Health (P50 MH100031; Dr. Richard Davidson) and R00 MH11056 (Dr. Douglas Dean) from the National Institute of Mental Health, National Institutes of Health. Infrastructure support was also provided, in part, by grant U54 HD090256 from the Eunice Kennedy Shriver NICHD, National Institutes of Health (Waisman Center) First author, Marissa DiPiero was also supported in part by NIH/NINDS T32 NS105602 and The Morse Society Graduate Student Fellowship for training in childhood mental health and developmental disabilities at the Waisman Center. The content is solely the responsibility of the authors and does not necessarily represent the official views of the National Institutes of Health.

Abstract

The neurodevelopmental epoch from fetal stages to early life embodies a critical window of peak growth and plasticity in which differences believed to be associated with many neurodevelopmental and psychiatric disorders first emerge. Obtaining a detailed understanding about the developmental patterns of the cortical gray matter microstructure is necessary to characterize differential patterns of neurodevelopment that may subserve future intellectual, behavioral, and psychiatric challenges. The NODDI Gray-Matter Based Spatial Statistics (GBSS) framework leverages information from the neurite orientation and dispersion density imaging (NODDI) model to enable sensitive characterization of the gray matter microstructure while limiting partial volume contamination and misregistration issues between images collected in different spaces. However, limited contrast of the underdeveloped brain poses challenges for implementing the NODDI-GBSS framework with infant diffusion MRI (dMRI) data. In this work, we examine infant cortical microstructure using GBSS and propose several refinements to the original framework that aim to improve the delineation and characterization of gray matter in the infant brain. Taking this approach, we cross-sectionally investigate age relationships in the developing gray matter microstructural organization in infants within the first month of life and reveal widespread relationships with the gray matter architecture.

Introduction

From early fetal stages to the first years of life, the brain undergoes immense morphological change that shapes its underlying structural and functional framework¹⁻⁴, providing the foundation for the development of future cognition and behavioral skills^{5, 6}. This developmental period of peak growth and neural plasticity encompasses a vulnerable window in which neurodevelopmental alterations believed to be associated with many neurodevelopmental and psychiatric disorders first emerge⁷⁻¹⁴. In particular, gray matter structures and associated cytoarchitecture help govern key neuronal processes supporting motor abilities, sensory integration, and cognitive functioning¹⁵⁻¹⁷ and are believed to play a critical role in various developmental conditions¹⁸⁻²². Therefore, understanding the early patterns of the brain's cortical development and organization is important to characterize normative development and detect diverging patterns of neurodevelopment that may be central to future intellectual, behavioral, and psychiatric challenges.

Quantitative magnetic resonance imaging (MRI) techniques such as diffusion MRI (dMRI) allow for in vivo characterization of the microstructural organization of the brain. dMRI probes tissue microstructure by quantitatively describing the random motion of water molecules in restricted tissue environments^{23, 24}. Diffusion tensor imaging (DTI) is the most widely used dMRI technique, enabling quantitative estimation of the brain's microstructure through four scalar indices: fractional anisotropy (FA), and mean (MD), radial (RD), and axial (AD) diffusivity. DTI metrics have been widely utilized in studies of neonatal white matter maturation²⁵⁻³⁰, however, DTI studies of infant gray matter have been largely limited and mostly studied in premature infants³¹⁻³⁴. Moreover, several limitations of the DTI model make it difficult to analyze and interpret DTI metrics in gray matter, including the assumption of a Gaussian diffusion distribution within the complex microstructure of the cortical gray matter³⁵ and bias from partial volume effects of the CSF³⁶. As such, considerable efforts toward developing alternative dMRI signal models have been made^{37, 38} including the development of biophysical models such as the neurite orientation and dispersion density imaging (NODDI)³⁹ model. Such models aim to improve the interpretation of the acquired dMRI signal and quantify characteristics of the brain's microstructure with enhanced biological specificity compared to traditional methods. NODDI metrics provide a quantitative estimation of neurite and axonal densities (FICVF), describe the extent of orientational dispersion of axonal projections (ODI), and estimate the fraction of free water CSF within a voxel (fISO)³⁹.

As early neurodevelopmental processes of the cortex including synaptogenesis, axon growth, and synaptic pruning, begin to lay the foundation for the brain's neural circuitry and shape the functional architecture of the brain⁵, it is critical to characterize the morphology of the emerging cytoarchitecture and define the developmental timing of these cortical processes. Despite the importance of understanding this microstructural development, few studies have applied advanced dMRI methods to assess cortical microstructural changes occurring in early brain development. This gap in literature is due to both challenges posed by incomplete white matter myelination and poor gray-white matter contrast in the underdeveloped brain⁴⁰⁻⁴² as well as the inherent difficulties of scanning infants and young children⁴³⁻⁴⁶.

NODDI metrics have been used in studies of early brain development to describe the organization of both white and gray matter regions⁴⁷⁻⁵³ showing widespread non-linear increases in FICVF⁵⁴⁻⁵⁶ and ODI⁵⁶ across development. Nevertheless, much of this extant work focuses on infants born pre-term and utilizes region-of-interest-based approaches that do not adequately account for regional developmental variations across the whole brain. For a comprehensive

review of applications of advanced dMRI in studies of brain development, see DiPiero et al. 2022²².

NODDI - Gray matter based spatial statistics (GBSS)⁵⁷ is a recent framework that utilizes information gleaned from the NODDI model to perform statistical analysis across a skeletonized representation of the gray matter microstructure, analogous to the white matter tract based spatial statistics approach⁵⁸. Methods described in Nazeri et al., 2017 allow for partial volume estimation maps of each tissue class to be derived within the native diffusion space, reducing the effects of partial volume contamination and improving sensitivity⁵⁷. The GBSS framework has been used in conjunction with NODDI in studies of autism^{18, 59}, schizophrenia and bipolar disorder⁵⁷, and mild cognitive impairment and Alzheimer's Disease⁶⁰. However, a key step of the GBSS framework involves the segmentation of the brain's tissue types, which can be challenging in the developing brain due to reduced tissue contrast and rapid development during the first years of life. Hence, the framework proposed by Nazeri et al., may not be directly adopted to studies in the infant brain. Three previous studies have utilized a GBSS approach to assess cortical microstructure in the infant brain^{33, 34, 61}, provide valuable insight into infant cortical microstructure, and demonstrate the utility of GBSS in the developing brain. However, these studies leverage anatomical images for tissue segmentation and spatial normalization and, therefore, require accurate registration between the anatomical and dMRI images.

The aim of the current work was to refine the NODDI - GBSS framework proposed by Nazeri et al. for the 1-month brain while only leveraging information from diffusion-weighted imaging data for processing and analysis. Taking this approach, we quantify DTI and NODDI measures across the cortical gray matter and assess associations of these measures with gestation corrected age. Although sex differences in white matter microstructure are minimally detected in neonates^{47, 62, 63}, we assessed potential sex differences in gray matter organization. Following previous literature of full-term infants in the first month of life, we anticipate that the organization of the gray matter will increase with age across much of the cortex and will not show differences between male and female infants in this early developmental period. We believe this infant optimized GBSS framework will enable improved dMRI measurements and characterization of the developing cortical microstructure and forge opportunities for large-scale investigations of the gray matter microstructure across the lifespan.

Methods

Participants

Recruitment for this study was conducted as part of a longitudinal study conducted at the University of Wisconsin–Madison investigating the brain and emotion development over the first two years of life. Extensive inclusion and exclusion criteria are described elsewhere^{47, 51-53, 64-66}. Briefly, 149 pregnant women were enrolled during the second trimester of pregnancy (<28 weeks' gestation). Inclusion criteria required mothers to be between 18 and 40 years of age, expecting a singleton birth, have no of previous diagnosis of major psychiatric conditions or major head trauma, no pre-existing neurological conditions, autoimmune disorders or infections during pregnancy, and had an uncomplicated childbirth. Infants were excluded postnatally if they were admitted into the neonatal intensive care unit (NICU) for medical care and/or if the infant was not discharged with the mother. All inclusionary criteria were confirmed with mothers prior to enrollment and were confirmed by study team via medical history questionnaires across the longitudinal study visits.

The current study utilizes dMRI from 91 infants (48 female; 43 male) scanned in the first month of life (Mean = 32.86 days, corrected for gestational age). Additional demographic information

can be found in **Table 1**. Parental consent was obtained from each participating family upon enrollment. All study procedures were approved by the Institutional Review Board at the University of Wisconsin – Madison.

Table 1. Participant Demographics

Sample Demographics	
N	91
Sex (F; M)	48:43
Infant Age at Scan (Gestation Corrected Days); Mean (SD) [Range]	32.86 (6.08) [18-50]
Infant Age at Scan (Post Menstrual Age (PMA) (weeks)); Mean (SD) [Range]	44.7 (0.86) [42.5 – 47.5]
Mother Age at Birth; Mean (SD) [Range]	32.92 (3.78) [20.12-41.06]
Infant Race	
White	82
Black	1
Asian	5
Native American	2
Missing/Not Reported	1

** $PMA (weeks) = \frac{(Gestational\ days + Chronological\ Age)}{7}$

MRI Data Acquisition

MRI visits were scheduled to align with infant's sleep schedule. Upon arrival, infants were fed and swaddled, and data were acquired during natural non-sedated sleep^{45, 46}. After infants were asleep, they were fit with ear protection, including ear plugs, MiniMuff® (Natus Medical Incorporated) neonatal noise attenuating ear covers, and white noise played through electrodynamic headphones (MR Confon, Germany) to limit the acoustic noise of the scan. To further limit the acoustic sound during the MRI and increase the likelihood of the infant remaining asleep, an acoustically optimized imaging protocol was designed that limited the peak gradient slew rates of the MRI pulse sequences to approximately 67% of their nominal value.

MRI data were acquired on a 3 Tesla General Electric MR750 Discovery scanner using a 32 channel receive-only head RF array coil (Nova Medical, Wakefield, MA). A three-shell diffusion weighted imaging (DWI) protocol was acquired using a single shot spin-echo echo-planar imaging pulse sequence. Parallel acquisition with a geometric reduction factor of two was used to reduce image acquisition time and distortions from magnetic field inhomogeneities. A total of 69 DWIs were acquired, 6 directions acquired with no diffusion weighting ($b = 0$ s/mm²), and diffusion weighting of $b = 350$ s/mm² in 9 directions, $b = 800$ s/mm² in 18 directions, and $b = 1500$ s/mm² in 36 directions. Other DWI acquisition parameters included a repetition time [TR] = 8400 ms; echo time [TE] = 94 ms; and bandwidth = 3906 Hz/pixel; field of view [FOV] of 25.6 cm × 25.6 cm and an acquisition matrix of 128 × 128, providing a 2mm × 2mm in-plane resolution. Coverage across the cerebrum and cerebellum was achieved by acquiring 60

sagittal-oriented contiguous slices with a slice thickness of 2.0 mm. The total time for the multiple b -value DTI acquisition using strategies to reduce the acoustic noise was approximately 10 minutes.

Structural T1- and T2-weighted images were obtained using GE's 3D BRAVO (BRAIn Volume) and CUBE imaging pulse sequences, respectively. Images were acquired in a sagittal orientation with a 1.0 mm isotropic spatial resolution. Additional BRAVO imaging parameters included: TR = 8.7 ms; TE = 3.4 ms; inversion time (TI) = 450 ms; flip angle = 12 degrees; FOV = 25.6 cm × 25.6 cm × 17.0 cm; and an acquisition time of 8 minutes 10 seconds. CUBE imaging parameters were: TR = 2500 ms; FOV = 25.6 cm × 25.6 cm × 16.0 cm; echo train length = 65; and an acquisition time of 5 minutes and 36 seconds.

Image Processing

All DWI and structural T1- and T2- weighted images were manually assessed for motion and other image artifacts and confirmed by a trained researcher (MD). DWI volumes containing motion artifacts were manually removed prior to processing. Data processing was conducted with an in-house processing pipeline. Briefly, DWIs were denoised⁶⁷ and corrected for Gibbs ringing artifact⁶⁸ using tools from MRtrix3⁶⁷. Eddy current and motion correction was performed using FSL's *eddy* tool⁶⁹⁻⁷², while gradient directions were further corrected for rotations⁷³. Non-parenchyma signal was removed using the *hd-bet*⁷⁴. DWIs were then up-sampled to 1mm³ isotropic resolution and linearly co-registered to the individuals' T2-weighted image using ANTs⁷⁵. Diffusion tensors were estimated at each voxel from the final pre-processed DWI image using a weighted-least squares algorithm using the Diffusion Imaging in Python (DIPY) package⁷⁶. DTI metrics^{77,78} including fractional anisotropy, and mean, radial, and axial diffusivities, (FA, MD, RD, AD) were computed. DWIs were also fit to the multi-compartment NODDI tissue model³⁹ with a Watson distribution using DMIPY⁷⁹ to estimate NODDI metrics of intracellular volume fraction (FICVF) or neurite density, orientation dispersion index (ODI), and isotropic volume fraction (FISO).

Adapting the GBSS Framework for Infants

NODDI-GBSS adopts the tract-based spatial statistics (TBSS)⁵⁸ framework to allow for analysis of diffusion MRI measures in the cortical gray matter. Processing steps for GBSS have been previously described^{57,80}. Briefly, the GBSS framework leverages the gray-white matter contrast of a DTI FA map for two-tissue type segmentation and estimation of the white matter fraction using Atropos⁸¹. A gray matter fraction map is then estimated by subtracting the white matter fraction and CSF fraction (NODDI FISO parameter) maps from 1. Gray matter fraction maps are then aligned to a study-specific template and averaged to create a representative gray matter fraction map. This map is then skeletonized using the *tbss_skeleton* tool in FSL^{58,82} and thresholded to include only voxels with an average gray matter fraction >0.65⁵⁷ (**Figure 1A**). NODDI and DTI metrics are projected onto the gray matter skeleton from local voxels with the greatest gray matter fraction.

The underdeveloped infant brain poses several challenges for the direct application of the NODDI-GBSS framework to infant dMRI data. For example, the FA contrast in infants is not sufficient for accurate gray and white matter segmentation and can result in erroneous estimates of the white matter fraction and, subsequently, the gray matter fraction (**Figure 1B**). This erroneous gray matter fraction estimation with the adult method causes further issues with the skeletonization of the gray matter as seen in **Figure 2B**.

To combat the suboptimal segmentation of the infant FA map, we propose using the NODDI ODI map for the two-tissue class segmentation and white matter fraction estimation due to its

improved gray-white matter contrast in the underdeveloped brain (**Figure 1C**). The gray matter fraction map was then estimated by subtracting the white matter fraction and CSF fraction (NODDI FISO parameter) maps from 1. Gray matter fraction maps are then aligned to a study-specific template, averaged to create a mean gray matter fraction map, and skeletonized using the *tbss_skeleton* tool in FSL^{58, 82}. However, due to the reduced gray matter fraction values in the 1-month brain, an adjusted gray matter fraction threshold of 0.45 was used to construct the infant gray matter skeleton (**Figure 2C**), which was used in subsequent statistical analyses. NODDI and DTI metrics were projected onto the gray matter skeleton from local voxels with the greatest gray matter fraction. To compare GM skeletonization methods performed in the infant brain, we examined the degree to which the two methods agreed with one another by calculating the percent agreement by dividing the number of agreeing (overlapping) voxels between methods by the total number of voxels in the infant skeleton.

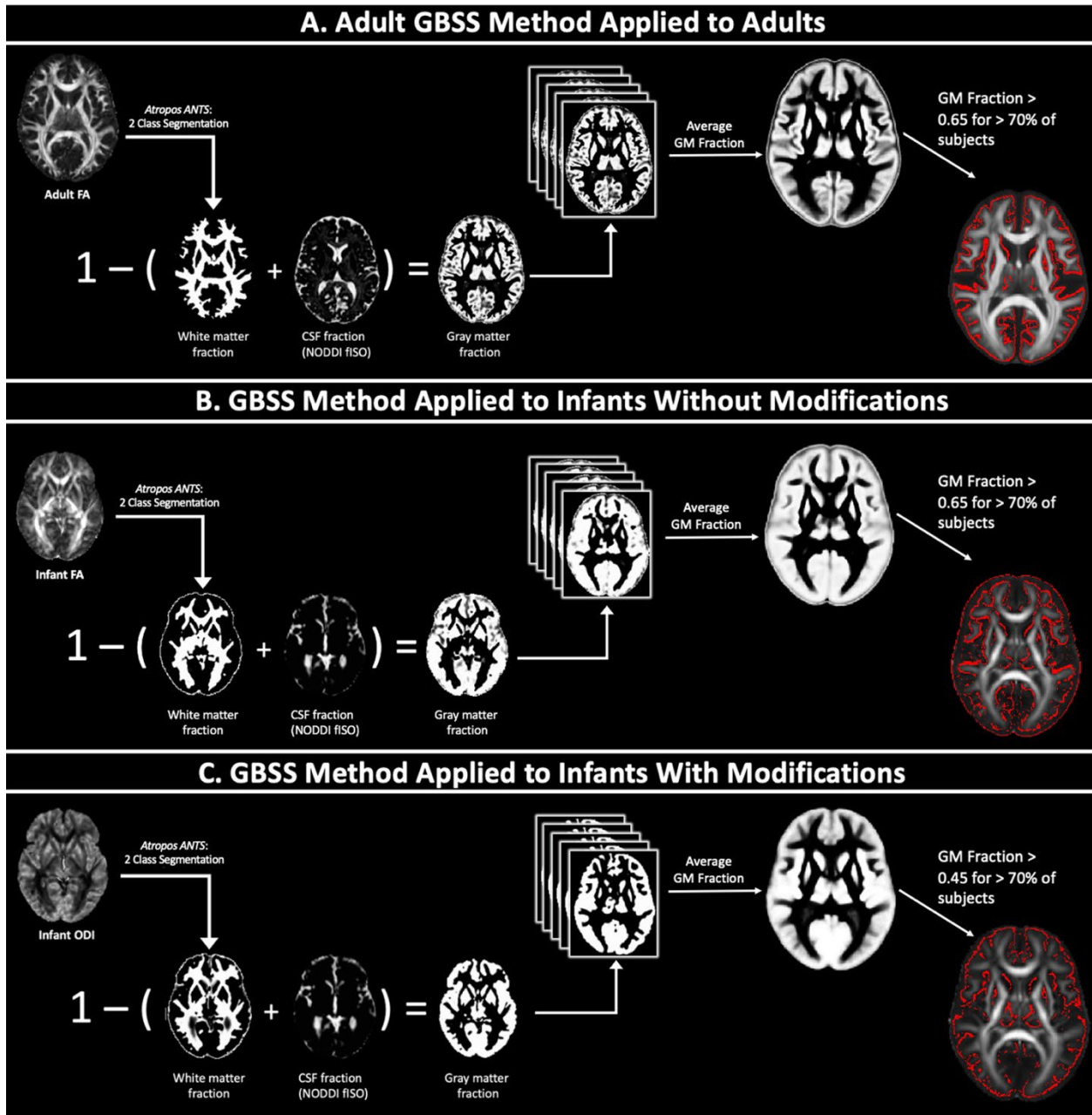


Figure 1. The GBSS Processing Steps Adapted to The Infant Brain. A. GBSS conducted in adults. For each subject, a white matter fraction map is estimated via Atropos from the DTI FA map. A gray matter fraction map is then generated by subtracting the white matter fraction and the CSF fraction (NODDI fISO) from 1. A mean gray matter fraction map is generated by averaging the gray matter fraction maps for each participant and is skeletonized. The dMRI parameter maps (from DTI and NODDI) are then projected onto the GM skeleton from the local gray matter fraction maxima. The final skeleton was generated by keeping only voxels with a GM fraction > 0.65 in $> 75\%$ of the subjects. **B. The adult optimized GBSS method applied directly to infants without modification.** The FA map was used to derive the white matter fraction estimate. The final skeleton was generated by keeping only voxels with a gray matter fraction > 0.65 in $> 75\%$ of the subjects leads to inaccuracies in gray matter fraction estimation and poor skeleton generation. **C. Modification of the GBSS framework for the infant brain.** For each subject, the NODDI ODI map was fed into Atropos for white matter fraction estimation. The final skeleton was generated by keeping only voxels with a gray matter fraction > 0.45 in $> 75\%$ of the subjects leads an improvement in gray matter fraction estimation and skeleton generation compared to the adult method in infants.

Statistical Analyses

Relationships with Age and Cortical Microstructure

FSL was used to build General Linear Models (GLMs) to investigate age relationships across the cortical microstructure. Infant age at scan was corrected for gestational age. Models controlled for infant sex. Covariates in all analyses were centered. Non-parametric permutation testing with tail approximation ($n = 500$) was carried out using Permutation Analysis of Linear Models (PALM)^{58, 83}. Tail approximation was used to fit the tail of the permutation distribution to a generalized Pareto distribution⁸⁴ and reduce the overall total number of permutations necessary to estimate p-values. A multivariate analysis was run for all gray matter metrics (FICVF, ODI, FA, MD, RD, AD). Joint inference of age was assessed with the non-parametric combination (NPC) and Fisher's combining function across five dMRI metrics: FICVF, FA, MD, AD, and RD, while differences in individual metrics were also evaluated. Threshold free cluster enhancement (TFCE)⁸⁵ was used to identify significant regions at $p < 0.05$, FWER-corrected across modality and contrast. Statistical maps were overlaid on the Harvard-Oxford cortical atlas⁸⁶ to identify regions with a significant age relationship.

Age by Sex Interactions on Cortical Microstructure

Age by sex interaction GLMs were also generated to separately examine sex related differences in the relationship between age and cortical organization. GLMs included mean-centered infant age (gestation corrected) and sex in addition to the interaction term. Non-parametric permutation testing with tail approximation ($n = 500$) was carried out using Permutation Analysis of Linear Models (PALM)^{58, 83}. Tail approximation was used to fit the tail of the permutation distribution to a generalized Pareto distribution⁸⁴ and reduce the overall total number of permutations necessary to estimate p-values. A multivariate analysis was run for all gray matter metrics (FICVF, ODI, FA, MD, RD, AD). Joint inference of age was assessed with the non-parametric combination (NPC) and Fisher's combining function across five dMRI metrics: FICVF, FA, MD, AD and RD, while differences in individual metrics were also evaluated. Threshold free cluster enhancement (TFCE)⁸⁵ was used to identify significant regions at $p < 0.05$, FWER-corrected across modality and contrast.

Results

GBSS Skeleton Construction for the Infant Brain

We show improved skeletonization of the gray matter microstructure in the infant brain with our adapted GBSS framework. Our modifications to the GBSS framework, including utilization of the NODDI ODI map for improved gray matter fraction estimate and adjusted threshold for generation of the gray matter skeleton (**Figure 1C**) contribute to an improved gray matter skeleton for infants (**Figure 2C**). When applying the GBSS framework directly to infants without these modifications, the resulting GM skeleton is centered at the gray-white matter boundary rather than within the cortical gray matter (**Figure 2B**). Moreover, we observe that erroneous segmentation of the DTI FA map results in inaccurate delineation of gray and white matter around the brain's edges (**Figure 2B**). The GBSS skeleton constructed via our infant adapted framework provides a more robust estimate of the gray matter fraction (**Figure 2C**) and generates a skeleton that is more specific to gray matter compared to the GBSS framework without modifications (**Figure 2B**). Further, the gray matter skeletons generated from both methods overlaid on one another highlight discrete regions of the brain (**Figure 2D**) with very few overlapping voxels in the cortex (**Figure 3**). Between the two GBSS approaches, only a 9.7% agreement was found between skeletonized voxels.

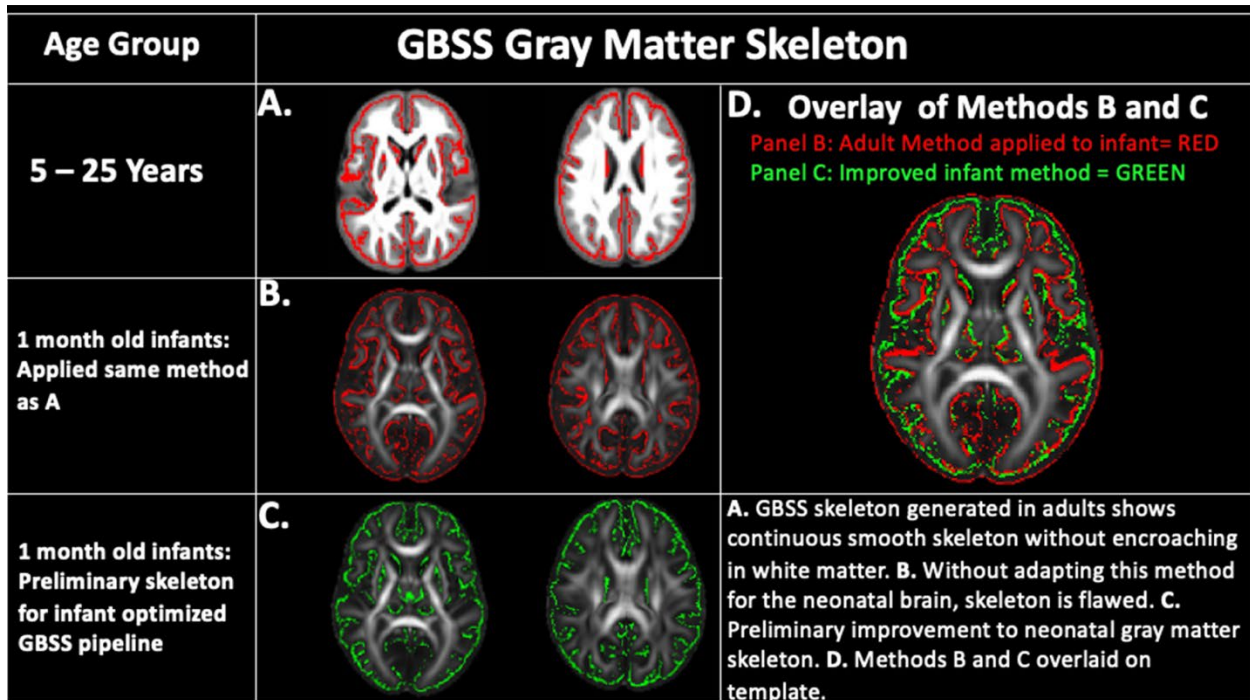


Figure 2: GBSS skeleton construction and improvement for infant brain. A. GBSS method applied to adult brain. B. GBSS method applied to infants without modification. C. Improved infant GBSS skeleton with adapted method. D. Adult GBSS method applied to infants without modification and infant GBSS method overlaid on top of one another.

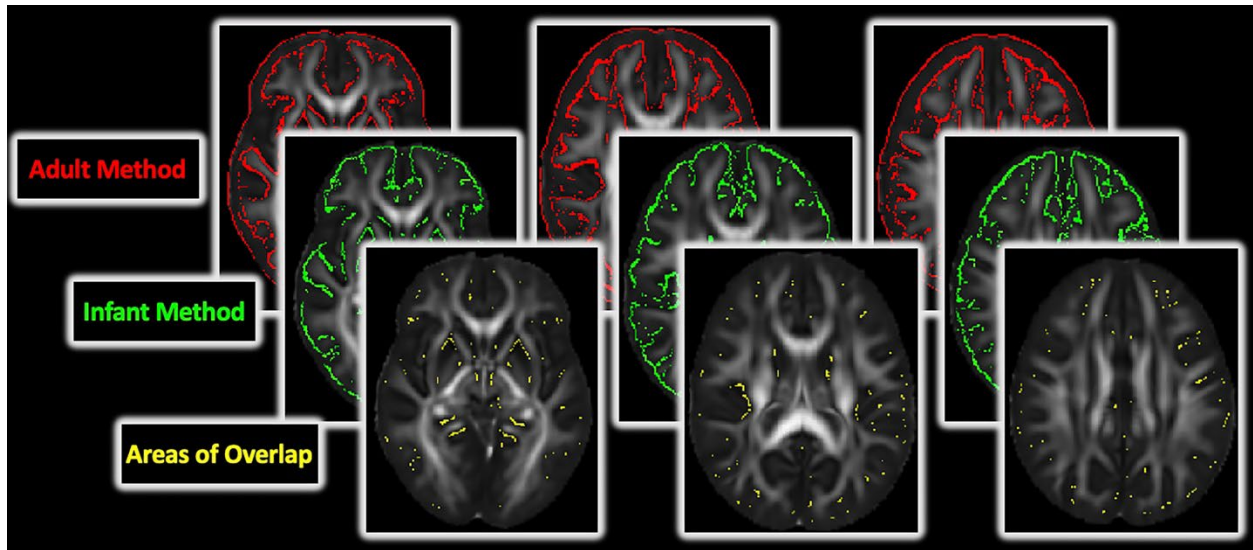


Figure 3. GBSS Skeleton Agreement Between Adult and Infant Methods. Yellow voxels represent voxels identified as gray matter across both the adult (Red) and infant (Green) methods.

Associations Between Cortical Microstructure and Age and Sex

A significant main effect of sex was not detected with cortical microstructure, however, age analyses controlled for the effects of sex. Significant voxelwise relationships with age and gray matter microstructure were observed in measures of FICVF, MD, RD, and AD ($p < 0.05$, FWER-corrected) (**Figure 3**). FICVF was observed to increase with age, whereas MD, RD and AD decreased with age. A summary of regional brain regions observed to have significant age relationships can be found in **Table 2**. Across significant dMRI metrics, age associations were observed in the cuneal cortex, lateral occipital cortex, occipital pole, paracingulate gyrus, cingulate gyrus, and the superior frontal gyrus. Across measures of FICVF, MD, and RD, significant age associations were also noted in the following regions: Angular gyrus, central opercular gyrus, inferior frontal gyrus, supplemental motor cortex, frontal pole, middle frontal gyrus, post central gyrus, precentral gyrus, supramarginal gyrus, and inferior temporal gyrus. While a majority of age relationships were found in bilateral hemispheres for FICVF, the majority of significant age relationships with the DTI metrics of MD and RD were found in the right hemisphere. Significant relationships between age and ODI were not detected across the cortical skeleton.

Across dMRI measures, we did not detect a significant main effect of sex or age-by-sex interactions in the cortical microstructure.

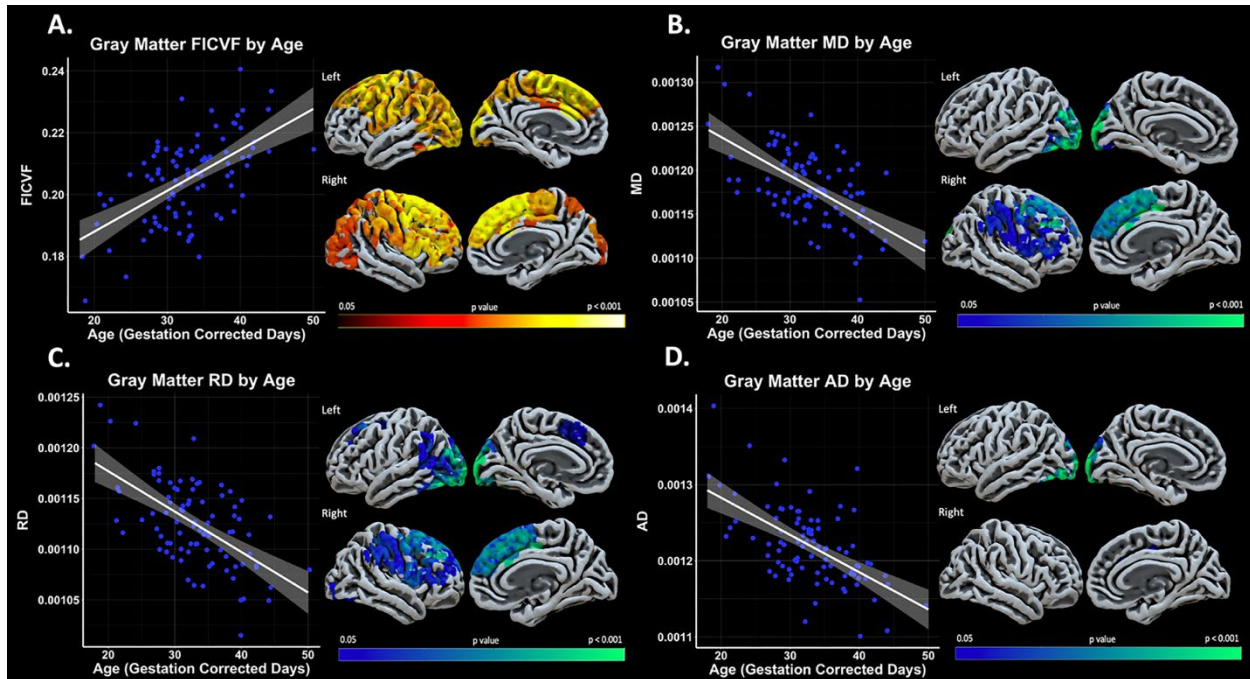


Figure 4. Age relationships in Cortical Microstructure. Neuroanatomical maps show regions with a significant age relationship. Color indicates level of significance. Red/Yellow scale indicates a significant positive relationship. Blue/Green scale indicates a significant negative relationship. Scatter points represent the average dMRI measure across significant voxels for each measure.

Discussion

The early organization of the cortical gray matter plays a critical role in the formation of the neural circuitry that is foundational for future behavioral health and well-being. Despite the importance of this early organization, limited work has applied advanced dMRI methods to investigate the highly complex and rapidly changing architecture of neurites in the cortex. This study employs GBSS⁵⁷ for characterizing the cortical microstructure and proposes several refinements to the original framework that aim to improve the delineation and characterization of gray matter in the infant brain. DTI and NODDI based measures of cortical microstructure were measured in the cortical gray matter and varied across much of the cortex, signaling rapid development and organization within the first month of life. These results complement the extant literature on the development of cortical microstructure and provide new insights into the neonatal brain.

Studies utilizing NODDI to examine the cortical organization of infants at 37 to 44 weeks post-menstrual age (PMA) show FICVF and ODI measured in the gray matter to increase with age^{56, 61, 87}, potentially capturing gray matter processes of dendritic arborization, glial proliferation, and synapse formation. Other work including older infants suggests a developmental plateau in gray matter organization around 38 weeks PMA^{54, 88}. For example, in a whole-brain gray matter analysis of preterm infants scanned between 25 and 47 weeks PMA, Batalle et al. reported a developmental plateau in ODI accompanied by an increase in FICVF after 38 PMW⁵⁴, suggesting the completion of basal dendritic branching and ongoing apical branching at this developmental stage^{54, 89}. However, dynamic cytoarchitectural changes continue into the neonatal period and within the first weeks of life including processes of neuronal aggregation in the formation of neural circuitry expanding both tangentially and radially⁹⁰. These

cytoarchitectural events may explain increases in FICVF and ODI in the gray matter of infants scanned between 37- and 44-weeks PMA^{56, 61}. In line with findings from Batalle et al., 2019⁵⁴, our observations of a rise in neurite density with age without a corresponding increase in dispersion may be attributed to ongoing apical dendritic development of pyramidal neurons at term-age⁹⁰⁻⁹².

Across the infant-modified GBSS skeleton, we detected significant relationships with age and gray matter microstructure measures of FICVF, MD, RD, and AD in brain regions including the cuneal cortex, lateral occipital cortex, occipital pole, paracingulate gyrus, cingulate gyrus, and the superior frontal gyrus. Within these regions, neurite density was positively associated with age, whereas the diffusivity metrics were negatively related to infant age. While the cuneal cortex, lateral occipital cortex, and occipital pole are located in the occipital lobe and play a major role in visual processes including interpreting visual stimuli⁹³, the paracingulate gyrus, cingulate gyrus, and the superior frontal gyrus are involved in cognitive and emotional processing^{94, 95}.

Early postnatal visual experiences influence the structural and functional maturation of the infant visual system⁹⁶. Our observation of microstructural development denoted by increased neurite density and decreased diffusivity metrics in these brain areas follows the expected developmental time course. Moreover, these neurite density changes complement findings from Batalle et al., 2019⁵⁴ in increased neurite density visual brain areas after 38 weeks PMA and is further supported by post-mortem histology findings of increased branching and spine densities at 1 month of age⁹⁷. Additional studies are needed to specifically link developing cortical microstructure to histology across developmental epochs.

The development of cognitive and emotional brain areas begins in infancy, with studies linking infant white matter microstructure of tracts supporting cognitive and emotional processes with future attentional⁵¹ and fear⁶⁵ behaviors. Neurite density of infant white matter tracts in frontal brain areas has also been shown to increase with age^{47, 98}. However, less work has specifically investigated these relationships in gray matter. Dimitrova et al., 2021 reported positive associations in FICVF with age in some regions of the frontal lobe of term-born neonates scanned between 37- and 44-weeks PMA⁵⁶. This work supports our findings of increased neurite density in the superior frontal gyrus and limbic brain structures. While other work also observed increased neurite density in the insula in infancy^{56, 61}, these studies included younger infants than represented in our sample which may account for the lack of findings in this region within our cohort.

Occurring in tandem with development in cognitive and emotional brain areas is the ongoing development of auditory and language centers. The development of hearing begins at the onset of the third trimester of pregnancy⁹⁹. Studies have shown that within the first postnatal months of life, infants already possess the ability to distinguish between different phonemes^{100, 101}. Moreover, studies have linked infant brain structure to later language abilities^{102, 103}, reporting relationships between subcortical gray matter densities and volumes and later language skills. The current work supports the early emergence of this protracted developmental process, with findings of increased neurite density and decreased mean and radial diffusivities observed within brain regions supporting phonetic and semantic language processes, including the middle frontal gyrus, inferior frontal gyrus, supramarginal gyrus, and angular gyrus.

In addition to language areas, we also observed an increase in structural organization in motor and sensory regions including the central opercular gyrus, supplemental motor regions, and the

pre-and post-central gyri. Findings from Fenchel et al., 2020 utilizing NODDI metrics and morphometric similarity networks highlighted sensory, limbic, and parietal brain areas to have the largest maturational change over the neonatal period compared to cognitive brain regions⁴⁹. These findings are consistent with histological findings of increased neurite density in this period in primary motor and sensory cortices⁹² and are further supported by diffusion MRI studies showing decreased diffusion anisotropy in sensorimotor cortices^{33, 104} and increased neurite density in sensory cortices⁵⁶.

In conclusion, our work is amongst the first to employ the GBSS framework in conjunction with NODDI metrics across the cortex in infants. With this framework adapted for neonatal brain, we forge opportunities to explore this maturation in expanded developmental epochs. Interpretation of our current work is limited by the cross-sectional design, limited sample diversity, and narrow age range of included infants. We encourage future work to utilize our current methods for exploring developmental patterns in more diverse samples of infants and across age ranges. Large-scale studies are currently underway including the “Developing Human Connectome Project¹⁰⁵”, “Baby Connectome Project¹⁰⁶”, and the “Healthy Brain and Child Development¹⁰⁷” study, building the potential for innovation in the understanding of human brain development from its earliest stages. The development and modification of advanced tools for probing cytoarchitectural maturation in the cortex in infancy, such as the current infant modified GBSS framework, paves the way for insights into the emergence of individual developmental differences that may underly future behavioral outcomes and creates room for the development of targeted interventions that promote the long-term health and well-being of children across the lifespan.

References

1. Thompson PM, Cannon TD, Narr KL, van Erp T, Poutanen V-P, Huttunen M, et al. Genetic influences on brain structure. *Nature Neuroscience*. 2001;4(12):1253-8.
2. Douet V, Chang L, Cloak C, Ernst T. Genetic influences on brain developmental trajectories on neuroimaging studies: from infancy to young adulthood. *Brain Imaging Behav*. 2014;8(2):234-50.
3. Teeuw J, Brouwer RM, Guimarães JPOFT, Brandner P, Koenis MMG, Swagerman SC, et al. Genetic and environmental influences on functional connectivity within and between canonical cortical resting-state networks throughout adolescent development in boys and girls. *NeuroImage*. 2019;202:116073.
4. Gao W, Elton A, Zhu H, Alcauter S, Smith JK, Gilmore JH, et al. Intersubject variability of and genetic effects on the brain's functional connectivity during infancy. *J Neurosci*. 2014;34(34):11288-96.
5. Ouyang M, Dubois J, Yu Q, Mukherjee P, Huang H. Delineation of early brain development from fetuses to infants with diffusion MRI and beyond. *Neuroimage*. 2019;185:836-50.
6. Steinberg L. Cognitive and affective development in adolescence. *Trends Cogn Sci*. 2005;9(2):69-74.
7. Rees S, Inder T. Fetal and neonatal origins of altered brain development. *Early Human Development*. 2005;81(9):753-61.
8. Bale TL, Baram TZ, Brown AS, Goldstein JM, Insel TR, McCarthy MM, et al. Early life programming and neurodevelopmental disorders. *Biol Psychiatry*. 2010;68(4):314-9.
9. De Asis-Cruz J, Andescavage N, Limperopoulos C. Adverse Prenatal Exposures and Fetal Brain Development: Insights From Advanced Fetal Magnetic Resonance Imaging. *Biological Psychiatry: Cognitive Neuroscience and Neuroimaging*. 2022;7(5):480-90.
10. Al-Haddad BJS, Oler E, Armistead B, Elsayed NA, Weinberger DR, Bernier R, et al. The fetal origins of mental illness. *Am J Obstet Gynecol*. 2019;221(6):549-62.
11. Oskvig DB, Elkahlon AG, Johnson KR, Phillips TM, Herkenham M. Maternal immune activation by LPS selectively alters specific gene expression profiles of interneuron migration and oxidative stress in the fetus without triggering a fetal immune response. *Brain Behav Immun*. 2012;26(4):623-34.
12. Smith KE, Pollak SD. Early life stress and development: potential mechanisms for adverse outcomes. *Journal of Neurodevelopmental Disorders*. 2020;12(1):34.
13. Hazlett HC, Gu H, Munsell BC, Kim SH, Styner M, Wolff JJ, et al. Early brain development in infants at high risk for autism spectrum disorder. *Nature*. 2017;542(7641):348-51.
14. Marín O. Developmental timing and critical windows for the treatment of psychiatric disorders. *Nature Medicine*. 2016;22(11):1229-38.
15. Arsalidou M, Duerden EG, Taylor MJ. The centre of the brain: Topographical model of motor, cognitive, affective, and somatosensory functions of the basal ganglia. *Human Brain Mapping*. 2013;34(11):3031-54.
16. Herrero MT, Barcia C, Navarro JM. Functional anatomy of thalamus and basal ganglia. *Childs Nerv Syst*. 2002;18(8):386-404.
17. Catani M, Dell'Acqua F, De Schotten MT. A revised limbic system model for memory, emotion and behaviour. *Neuroscience & Biobehavioral Reviews*. 2013;37(8):1724-37.

18. DiPiero M, Cordash H, Prigge MB, King CK, Morgan J, Guerrero-Gonzalez J, et al. Tract- and gray matter- based spatial statistics show white matter and gray matter microstructural differences in autistic males. *Frontiers in Neuroscience*. 2023;17.
19. Rogers CE, Barch DM, Sylvester CM, Pagliaccio D, Harms MP, Botteron KN, et al. Altered gray matter volume and school age anxiety in children born late preterm. *J Pediatr*. 2014;165(5):928-35.
20. Batty MJ, Liddle EB, Pitiot A, Toro R, Groom MJ, Scerif G, et al. Cortical gray matter in attention-deficit/hyperactivity disorder: a structural magnetic resonance imaging study. *J Am Acad Child Adolesc Psychiatry*. 2010;49(3):229-38.
21. Tomohiro Nakao, M.D., Ph.D. , Joaquim Radua, M.D. , Katya Rubia, Ph.D. , and, David Mataix-Cols, Ph.D. Gray Matter Volume Abnormalities in ADHD: Voxel-Based Meta-Analysis Exploring the Effects of Age and Stimulant Medication. *American Journal of Psychiatry*. 2011;168(11):1154-63.
22. DiPiero M, Rodrigues PG, Gromala A, Dean DC. Applications of advanced diffusion MRI in early brain development: a comprehensive review. *Brain Structure and Function*. 2022.
23. Afzali M, Pieciak T, Newman S, Garyfallidis E, Ozarslan E, Cheng H, et al. The sensitivity of diffusion MRI to microstructural properties and experimental factors. *J Neurosci Methods*. 2021;347:108951.
24. Basser PJ, Ozarslan E. Introduction to Diffusion MR. *Diffusion Mri: From Quantitative Measurement to in Vivo Neuroanatomy*. 2009:3-10.
25. Qiu A, Mori S, Miller MI. Diffusion tensor imaging for understanding brain development in early life. *Annu Rev Psychol*. 2015;66:853-76.
26. Gao W, Lin W, Chen Y, Gerig G, Smith JK, Jewells V, et al. Temporal and spatial development of axonal maturation and myelination of white matter in the developing brain. *AJNR Am J Neuroradiol*. 2009;30(2):290-6.
27. Geng X, Gouttard S, Sharma A, Gu H, Styner M, Lin W, et al. Quantitative tract-based white matter development from birth to age 2years. *Neuroimage*. 2012;61(3):542-57.
28. Stephens RL, Langworthy BW, Short SJ, Girault JB, Styner MA, Gilmore JH. White Matter Development from Birth to 6 Years of Age: A Longitudinal Study. *Cereb Cortex*. 2020;30(12):6152-68.
29. Cancelliere A, Mangano FT, Air EL, Jones BV, Altaye M, Rajagopal A, et al. DTI Values in Key White Matter Tracts from Infancy through Adolescence. *American Journal of Neuroradiology*. 2013;34(7):1443.
30. Dubois J, Dehaene-Lambertz G, Perrin M, Mangin JF, Cointepas Y, Duchesnay E, et al. Asynchrony of the early maturation of white matter bundles in healthy infants: quantitative landmarks revealed noninvasively by diffusion tensor imaging. *Hum Brain Mapp*. 2008;29(1):14-27.
31. Lean RE, Han RH, Smyser TA, Kenley JK, Shimony JS, Rogers CE, et al. Altered neonatal white and gray matter microstructure is associated with neurodevelopmental impairments in very preterm infants with high-grade brain injury. *Pediatr Res*. 2019;86(3):365-74.
32. Bouyssi-Kobar M, Brossard-Racine M, Jacobs M, Murnick J, Chang T, Limperopoulos C. Regional microstructural organization of the cerebral cortex is affected by preterm birth. *Neuroimage Clin*. 2018;18:871-80.

33. Ball G, Srinivasan L, Aljabar P, Counsell SJ, Durighel G, Hajnal JV, et al. Development of cortical microstructure in the preterm human brain. *Proc Natl Acad Sci U S A*. 2013;110(23):9541-6.
34. Kelly CJ, Christiaens D, Batalle D, Makropoulos A, Cordero-Grande L, Steinweg JK, et al. Abnormal Microstructural Development of the Cerebral Cortex in Neonates With Congenital Heart Disease Is Associated With Impaired Cerebral Oxygen Delivery. *J Am Heart Assoc*. 2019;8(5):e009893.
35. Wheeler-Kingshott CA, Cercignani M. About "axial" and "radial" diffusivities. *Magn Reson Med*. 2009;61(5):1255-60.
36. Alexander AL, Hasan KM, Lazar M, Tsuruda JS, Parker DL. Analysis of partial volume effects in diffusion-tensor MRI. *Magn Reson Med*. 2001;45(5):770-80.
37. Alexander DC, Dyrby TB, Nilsson M, Zhang H. Imaging brain microstructure with diffusion MRI: practicality and applications. *NMR Biomed*. 2019;32(4):e3841.
38. Novikov DS, Fieremans E, Jespersen SN, Kiselev VG. Quantifying brain microstructure with diffusion MRI: Theory and parameter estimation. *NMR in Biomedicine*. 2019;32(4):e3998.
39. Zhang H, Schneider T, Wheeler-Kingshott CA, Alexander DC. NODDI: practical in vivo neurite orientation dispersion and density imaging of the human brain. *Neuroimage*. 2012;61(4):1000-16.
40. Dubois J, Alison M, Counsell SJ, Hertz-Pannier L, Huppi PS, Benders M. MRI of the Neonatal Brain: A Review of Methodological Challenges and Neuroscientific Advances. *J Magn Reson Imaging*. 2021;53(5):1318-43.
41. Wang L, Gao Y, Shi F, Li G, Gilmore JH, Lin W, et al. LINKS: Learning-based multi-source IntegratioN framework for Segmentation of infant brain images. *NeuroImage*. 2015;108:160-72.
42. Dubois J, Dehaene-Lambertz G, Kulikova S, Poupon C, Huppi PS, Hertz-Pannier L. The early development of brain white matter: a review of imaging studies in fetuses, newborns and infants. *Neuroscience*. 2014;276:48-71.
43. Hendrix CL, Thomason ME. A survey of protocols from 54 infant and toddler neuroimaging research labs. *Developmental Cognitive Neuroscience*. 2022;54:101060.
44. Raschle N, Zuk J, Ortiz-Mantilla S, Sliva DD, Franceschi A, Grant PE, et al. Pediatric neuroimaging in early childhood and infancy: challenges and practical guidelines. *Ann N Y Acad Sci*. 2012;1252:43-50.
45. Dean DC, 3rd, Dirks H, O'Muircheartaigh J, Walker L, Jerskey BA, Lehman K, et al. Pediatric neuroimaging using magnetic resonance imaging during non-sedated sleep. *Pediatr Radiol*. 2014;44(1):64-72.
46. Spann MN, Wisnowski JL, Smyser CD, Howell B, Dean DC, 3rd. The Art, Science, and Secrets of Scanning Young Children. *Biol Psychiatry*. 2022.
47. Dean DC, 3rd, Planalp EM, Wooten W, Adluru N, Kecskemeti SR, Frye C, et al. Mapping White Matter Microstructure in the One Month Human Brain. *Sci Rep*. 2017;7(1):9759.
48. Stoye DQ, Blesa M, Sullivan G, Galdi P, Lamb GJ, Black GS, et al. Maternal cortisol is associated with neonatal amygdala microstructure and connectivity in a sexually dimorphic manner. *Elife*. 2020;9.
49. Fenchel D, Dimitrova R, Seidlitz J, Robinson EC, Batalle D, Hutter J, et al. Development of Microstructural and Morphological Cortical Profiles in the Neonatal Brain. *Cereb Cortex*. 2020;30(11):5767-79.

50. Kunz N, Zhang H, Vasung L, O'Brien KR, Assaf Y, Lazeyras F, et al. Assessing white matter microstructure of the newborn with multi-shell diffusion MRI and biophysical compartment models. *Neuroimage*. 2014;96:288-99.
51. Dowe KN, Planalp EM, Dean DC, 3rd, Alexander AL, Davidson RJ, Goldsmith HH. Early microstructure of white matter associated with infant attention. *Dev Cogn Neurosci*. 2020;45:100815.
52. Dean DC, 3rd, Planalp EM, Wooten W, Kecskemeti SR, Adluru N, Schmidt CK, et al. Association of Prenatal Maternal Depression and Anxiety Symptoms With Infant White Matter Microstructure. *JAMA Pediatr*. 2018;172(10):973-81.
53. Dean DC, 3rd, Planalp EM, Wooten W, Schmidt CK, Kecskemeti SR, Frye C, et al. Investigation of brain structure in the 1-month infant. *Brain Struct Funct*. 2018;223(4):1953-70.
54. Batalle D, O'Muircheartaigh J, Makropoulos A, Kelly CJ, Dimitrova R, Hughes EJ, et al. Different patterns of cortical maturation before and after 38 weeks gestational age demonstrated by diffusion MRI in vivo. *Neuroimage*. 2019;185:764-75.
55. Wang H, Ma Z-H, Xu L-Z, Yang L, Ji Z-Z, Tang X-Z, et al. Developmental brain structural atypicalities in autism: a voxel-based morphometry analysis. *Child and Adolescent Psychiatry and Mental Health*. 2022;16(1):7.
56. Dimitrova R, Pietsch M, Ciarrusta J, Fitzgibbon SP, Williams LZJ, Christiaens D, et al. Preterm birth alters the development of cortical microstructure and morphology at term-equivalent age. *Neuroimage*. 2021;243:118488.
57. Nazeri A, Mulsant BH, Rajji TK, Levesque ML, Pipitone J, Stefanik L, et al. Gray Matter Neuritic Microstructure Deficits in Schizophrenia and Bipolar Disorder. *Biol Psychiatry*. 2017;82(10):726-36.
58. Smith SM, Jenkinson M, Johansen-Berg H, Rueckert D, Nichols TE, Mackay CE, et al. Tract-based spatial statistics: voxelwise analysis of multi-subject diffusion data. *Neuroimage*. 2006;31(4):1487-505.
59. DiPiero MA, Sargent OJ, Travers BG, Alexander AL, Lainhart JE, Dean DC. Gray matter microstructure differences in autistic males: A gray matter based spatial statistics study. *Neuroimage Clin*. 2022;37:103306.
60. Vogt NM, Hunt JF, Adluru N, Dean DC, Johnson SC, Asthana S, et al. Cortical Microstructural Alterations in Mild Cognitive Impairment and Alzheimer's Disease Dementia. *Cereb Cortex*. 2020;30(5):2948-60.
61. Wang W, Yu Q, Liang W, Xu F, Li Z, Tang Y, et al. Altered cortical microstructure in preterm infants at term-equivalent age relative to term-born neonates. *Cereb Cortex*. 2022.
62. Liu Y, Metens T, Absil J, De Maertelaer V, Balériaux D, David P, et al. Gender differences in language and motor-related fibers in a population of healthy preterm neonates at term-equivalent age: a diffusion tensor and probabilistic tractography study. *American Journal of Neuroradiology*. 2011;32(11).
63. Gilmore JH, Knickmeyer RC, Gao W. Imaging structural and functional brain development in early childhood. *Nat Rev Neurosci*. 2018;19(3):123-37.
64. Dean DC, 3rd, Madrid A, Planalp EM, Moody JF, Papale LA, Knobel KM, et al. Cord blood DNA methylation modifications in infants are associated with white matter microstructure in the context of prenatal maternal depression and anxiety. *Sci Rep*. 2021;11(1):12181.
65. Planalp EM, Dowe KN, Alexander AL, Goldsmith HH, Davidson RJ, Dean III DC. White matter microstructure predicts individual differences in infant fear (But not anger and sadness). *Developmental Science*. 2023;26(3):e13340.

66. Birn RM, Dean DC, Wooten W, Planalp EM, Kecskemeti S, Alexander AL, et al. Reduction of Motion Artifacts in Functional Connectivity Resulting from Infrequent Large Motion. *Brain Connectivity*. 2022;12(8):740-53.
67. Tournier JD, Smith R, Raffelt D, Tabbara R, Dhollander T, Pietsch M, et al. MRtrix3: A fast, flexible and open software framework for medical image processing and visualisation. *Neuroimage*. 2019;202:116137.
68. Kellner E, Dhital B, Kiselev VG, Reisert M. Gibbs-ringing artifact removal based on local subvoxel-shifts. *Magn Reson Med*. 2016;76(5):1574-81.
69. Jenkinson M, Bannister P, Brady M, Smith S. Improved optimization for the robust and accurate linear registration and motion correction of brain images. *Neuroimage*. 2002;17(2):825-41.
70. Andersson JLR, Graham MS, Drobnyak I, Zhang H, Filippini N, Bastiani M. Towards a comprehensive framework for movement and distortion correction of diffusion MR images: Within volume movement. *Neuroimage*. 2017;152:450-66.
71. Andersson JLR, Sotiropoulos SN. An integrated approach to correction for off-resonance effects and subject movement in diffusion MR imaging. *Neuroimage*. 2016;125:1063-78.
72. Andersson JLR, Graham MS, Zsoldos E, Sotiropoulos SN. Incorporating outlier detection and replacement into a non-parametric framework for movement and distortion correction of diffusion MR images. *Neuroimage*. 2016;141:556-72.
73. Leemans A, Jones DK. The B-matrix must be rotated when correcting for subject motion in DTI data. *Magn Reson Med*. 2009;61(6):1336-49.
74. Isensee F, Schell M, Pflueger I, Brugnara G, Bonekamp D, Neuberger U, et al. Automated brain extraction of multisequence MRI using artificial neural networks. *Human Brain Mapping*. 2019;40(17):4952-64.
75. Avants BB, Tustison N, Song G. Advanced normalization tools (ANTs). *Insight j*. 2009;2(365):1-35.
76. Garyfallidis E, Brett M, Amirbekian B, Rokem A, van der Walt S, Descoteaux M, et al. Dipy, a library for the analysis of diffusion MRI data. *Front Neuroinform*. 2014;8:8.
77. Basser PJ. Inferring microstructural features and the physiological state of tissues from diffusion-weighted images. *NMR Biomed*. 1995;8(7-8):333-44.
78. Basser PJ, Pierpaoli C. Microstructural and physiological features of tissues elucidated by quantitative-diffusion-tensor MRI. *J Magn Reson B*. 1996;111(3):209-19.
79. Fick RHJ, Wassermann D, Deriche R. The Dmipy Toolbox: Diffusion MRI Multi-Compartment Modeling and Microstructure Recovery Made Easy. *Frontiers in Neuroinformatics*. 2019;13.
80. Nazeri A, Chakravarty MM, Rotenberg DJ, Rajji TK, Rathi Y, Michailovich OV, et al. Functional consequences of neurite orientation dispersion and density in humans across the adult lifespan. *J Neurosci*. 2015;35(4):1753-62.
81. Avants BB, Tustison NJ, Wu J, Cook PA, Gee JC. An open source multivariate framework for n-tissue segmentation with evaluation on public data. *Neuroinformatics*. 2011;9(4):381-400.
82. Jenkinson M, Beckmann CF, Behrens TE, Woolrich MW, Smith SM. Fsl. *Neuroimage*. 2012;62(2):782-90.
83. Winkler AM, Ridgway GR, Webster MA, Smith SM, Nichols TE. Permutation inference for the general linear model. *Neuroimage*. 2014;92:381-97.

84. James P, III. Statistical Inference Using Extreme Order Statistics. *The Annals of Statistics*. 1975;3(1):119-31.
85. Smith SM, Nichols TE. Threshold-free cluster enhancement: addressing problems of smoothing, threshold dependence and localisation in cluster inference. *Neuroimage*. 2009;44(1):83-98.
86. Desikan RS, Ségonne F, Fischl B, Quinn BT, Dickerson BC, Blacker D, et al. An automated labeling system for subdividing the human cerebral cortex on MRI scans into gyral based regions of interest. *Neuroimage*. 2006;31(3):968-80.
87. Eaton-Rosen Z, Melbourne A, Orasanu E, Cardoso MJ, Modat M, Bainbridge A, et al. Longitudinal measurement of the developing grey matter in preterm subjects using multi-modal MRI. *Neuroimage*. 2015;111:580-9.
88. Ouyang M, Jeon T, Sotiras A, Peng Q, Mishra V, Halovanic C, et al. Differential cortical microstructural maturation in the preterm human brain with diffusion kurtosis and tensor imaging. *Proc Natl Acad Sci U S A*. 2019;116(10):4681-8.
89. Mrzljak L, Uylings HBM, Kostovic I, van Eden CG. Prenatal development of neurons in the human prefrontal cortex: I. A qualitative Golgi study. *Journal of Comparative Neurology*. 1988;271(3):355-86.
90. Kostović I, Sedmak G, Judaš M. Neural histology and neurogenesis of the human fetal and infant brain. *NeuroImage*. 2019;188:743-73.
91. Becker LE, Armstrong DL, Chan F, Wood MM. Dendritic development in human occipital cortical neurons. *Developmental Brain Research*. 1984;13(1):117-24.
92. Huttenlocher PR. Morphometric study of human cerebral cortex development. *Neuropsychologia*. 1990;28(6):517-27.
93. Uysal S. The Occipital Lobes and Visual Processing. 2023 [cited 1/15/2024]. In: *Functional Neuroanatomy and Clinical Neuroscience: Foundations for Understanding Disorders of Cognition and Behavior* [Internet]. Oxford University Press, [cited 1/15/2024]; [168C14]. Available from: <https://doi.org/10.1093/oso/9780190943608.003.0014>.
94. Rolls ET. The cingulate cortex and limbic systems for emotion, action, and memory. *Brain Struct Funct*. 2019;224(9):3001-18.
95. Boisgheueuc Fd, Levy R, Volle E, Seassau M, Duffau H, Kinkingnehun S, et al. Functions of the left superior frontal gyrus in humans: a lesion study. *Brain*. 2006;129(12):3315-28.
96. Li M, Liu T, Xu X, Wen Q, Zhao Z, Dang X, et al. Development of visual cortex in human neonates is selectively modified by postnatal experience. *eLife*. 2022;11:e78733.
97. Takashima S, Chan F, Becker LE, Armstrong DL. Morphology of the Developing Visual Cortex of the Human Infant: A Quantitative and Qualitative Golgi Study. *Journal of Neuropathology & Experimental Neurology*. 1980;39(4):487-501.
98. Kimpton JA, Bataille D, Barnett ML, Hughes EJ, Chew ATM, Falconer S, et al. Diffusion magnetic resonance imaging assessment of regional white matter maturation in preterm neonates. *Neuroradiology*. 2021;63(4):573-83.
99. Granier-Deferre C, Ribeiro A, Jacquet AY, Bassereau S. Near-term fetuses process temporal features of speech. *Developmental science*. 2011;14(2):336-52.
100. Dehaene-Lambertz G, Pena M. Electrophysiological evidence for automatic phonetic processing in neonates. *Neuroreport*. 2001;12(14):3155-8.

101. Cheour-Luhtanen M, Alho K, Kujala T, Sainio K, Reinikainen K, Renlund M, et al. Mismatch negativity indicates vowel discrimination in newborns. *Hearing research*. 1995;82(1):53-8.
102. Deniz Can D, Richards T, Kuhl PK. Early gray-matter and white-matter concentration in infancy predict later language skills: a whole brain voxel-based morphometry study. *Brain Lang*. 2013;124(1):34-44.
103. Ortiz-Mantilla S, Choe M-s, Flax J, Grant PE, Benasich AA. Associations between the size of the amygdala in infancy and language abilities during the preschool years in normally developing children. *Neuroimage*. 2010;49(3):2791-9.
104. deIpoli AR, Mukherjee P, Gill K, Henry RG, Partridge SC, Veeraraghavan S, et al. Comparing microstructural and macrostructural development of the cerebral cortex in premature newborns: Diffusion tensor imaging versus cortical gyration. *NeuroImage*. 2005;27(3):579-86.
105. Edwards AD, Rueckert D, Smith SM, Abo Seada S, Alansary A, Almalbis J, et al. The Developing Human Connectome Project Neonatal Data Release. *Front Neurosci*. 2022;16:886772.
106. Howell BR, Styner MA, Gao W, Yap PT, Wang L, Baluyot K, et al. The UNC/UMN Baby Connectome Project (BCP): An overview of the study design and protocol development. *Neuroimage*. 2019;185:891-905.
107. Volkow ND, Gordon JA, Freund MP. The Healthy Brain and Child Development Study—Shedding Light on Opioid Exposure, COVID-19, and Health Disparities. *JAMA Psychiatry*. 2021;78(5):471-2.